



**HAL**  
open science

## Efficient storage mechanisms for building better supercapacitors

Mathieu Salanne, Benjamin Rotenberg, Katsuhiko Naoi, Katsumi Kaneko, Pierre-Louis Taberna, Clare P. Grey, Bruce Dunn, Patrice Simon

► **To cite this version:**

Mathieu Salanne, Benjamin Rotenberg, Katsuhiko Naoi, Katsumi Kaneko, Pierre-Louis Taberna, et al.. Efficient storage mechanisms for building better supercapacitors. *Nature Energy*, 2016, vol. 1, pp. 1-10. 10.1038/nenergy.2016.70 . hal-01480941v2

**HAL Id: hal-01480941**

**<https://hal.science/hal-01480941v2>**

Submitted on 10 Mar 2017

**HAL** is a multi-disciplinary open access archive for the deposit and dissemination of scientific research documents, whether they are published or not. The documents may come from teaching and research institutions in France or abroad, or from public or private research centers.

L'archive ouverte pluridisciplinaire **HAL**, est destinée au dépôt et à la diffusion de documents scientifiques de niveau recherche, publiés ou non, émanant des établissements d'enseignement et de recherche français ou étrangers, des laboratoires publics ou privés.



## Open Archive TOULOUSE Archive Ouverte (OATAO)

OATAO is an open access repository that collects the work of Toulouse researchers and makes it freely available over the web where possible.

This is an author-deposited version published in : <http://oatao.univ-toulouse.fr/>  
Eprints ID : 16758

**To link to this article** : DOI:10.1038/NENERGY.2016.70  
URL : <http://dx.doi.org/10.1038/NENERGY.2016.70>

<p><b>To cite this version</b> : Salanne, Mathieu and Rotenberg, Benjamin and Naoi, Katsuhiko and Kaneko, Katsumi and Taberna, Pierre-Louis and Grey, Clare P. and Dunn, Bruce and Simon, Patrice <i>Efficient storage mechanisms for building better supercapacitors.</i> (2016) Nature Energy, vol. 1. pp. 1-10. ISSN 2058-7546</p>
---

Any correspondence concerning this service should be sent to the repository administrator: [staff-oatao@listes-diff.inp-toulouse.fr](mailto:staff-oatao@listes-diff.inp-toulouse.fr)

# Efficient storage mechanisms for building better supercapacitors

M. Salanne<sup>1,2,3</sup>, B. Rotenberg<sup>1,2</sup>, K. Naoi<sup>4</sup>, K. Kaneko<sup>5</sup>, P.-L. Taberna<sup>2,6</sup>, C. P. Grey<sup>7</sup>, B. Dunn<sup>8</sup> and P. Simon<sup>2,4,6\*</sup>

**Supercapacitors are electrochemical energy storage devices that operate on the simple mechanism of adsorption of ions from an electrolyte on a high-surface-area electrode. Over the past decade, the performance of supercapacitors has greatly improved, as electrode materials have been tuned at the nanoscale and electrolytes have gained an active role, enabling more efficient storage mechanisms. In porous carbon materials with subnanometre pores, the desolvation of the ions leads to surprisingly high capacitances. Oxide materials store charge by surface redox reactions, leading to the pseudocapacitive effect. Understanding the physical mechanisms underlying charge storage in these materials is important for further development of supercapacitors. Here we review recent progress, from both *in situ* experiments and advanced simulation techniques, in understanding the charge storage mechanism in carbon- and oxide-based supercapacitors. We also discuss the challenges that still need to be addressed for building better supercapacitors.**

The urgent need for efficient energy storage devices has resulted in a widespread and concerted research effort into electrochemical capacitors, also called supercapacitors, in the past ten years. These devices consist of two high-conductivity electrodes separated by an electrolyte containing mobile ionic species. As in conventional capacitors, charge is stored at the surface of the electrodes through an excess of electrons on one side of the device and electron holes on the other side, on application of a voltage between the electrodes<sup>1</sup>. Unlike conventional capacitors, however, the charge on the electrodes is then balanced by the adsorption of cations and anions, respectively, at their surface. The excellent performance of supercapacitors is due to the highly reversible ion adsorption mechanism. In contrast to batteries, charging is not limited by diffusion of ions in the bulk of the electrodes, and hence higher power densities can be achieved. Supercapacitors can therefore complement and sometimes even replace batteries when high power delivery or uptake is needed<sup>2</sup>.

Two distinct families of supercapacitors can be considered. The principal one, electrochemical double-layer capacitors (EDLCs), uses porous carbon electrodes with high accessible surface area. This acts as an 'electric sponge', which adsorbs the ions from the electrolytes on charging and releases them at discharge. After years of incremental developments, the discovery of a different charging mechanism in nanoporous carbons (with pore size smaller than 1 nm) has spurred further research into EDLCs<sup>3</sup>. As a consequence, recent work has not only been directed towards new materials and architectures, but is also aimed at understanding the physical mechanisms underlying the charge storage in such materials. The development of *in situ* experiments, in particular spectroscopy and diffraction, as well as advanced simulation techniques for the realistic description of complex interfacial

processes, has radically modified our understanding of nanoporous carbon-based supercapacitors.

The second family of supercapacitors, known as pseudocapacitors, is based on redox reactions that occur largely (but not exclusively) on oxide-based material surfaces<sup>4</sup>. Fundamental studies on pseudocapacitors remain scarce, because of the difficulty of characterizing the oxide surfaces and determining the details of the charge transfer mechanism. But the recent development of nanostructured oxides and of hybrid carbon/oxide electrodes is progressively changing the way we think about pseudocapacitive charge storage.

Despite the recent progress in both the performance and fundamental understanding of the mechanisms involved in supercapacitors, this body of work has not been placed in the broader context of capacitive storage. Existing reviews in the literature either focus on the properties of the materials<sup>5-7</sup> or on the electrolytes<sup>8,9</sup>. Here we review both chemical and physical aspects of the capacitive storage mechanism in carbon- and oxide-based supercapacitors. We discuss the latest advances, which have implications not only for supercapacitors but also for other applications in which voltage-driven ion adsorption in nanoporous structures plays a key role.

## Electrochemical double-layer capacitors

Charge storage in supercapacitor electrodes makes use of the electrostatic attraction between the ions of an electrolyte and the charges present at the electrode surface, which allows the formation of oppositely charged layers at the electrolyte/electrode interface. Supercapacitors use mainly porous carbon as electrode materials, thus benefiting from the high surface area available for ion adsorption. The charge separation occurring upon polarization at the electrode/electrolyte interface can be described in a crude approach

<sup>1</sup>Sorbonne Universités, UPMC Univ. Paris 06, CNRS, Laboratoire PHENIX, F-75005 Paris, France. <sup>2</sup>Réseau sur le Stockage Electrochimique de l'Energie (RS2E), FR CNRS 3459, 80039 Amiens Cedex, France. <sup>3</sup>Maison de la Simulation, USR 3441, CEA, CNRS, INRIA, Université Paris-Sud, Université de Versailles, F-91191 Gif-sur-Yvette, France. <sup>4</sup>Institute of Global Innovation Research, Tokyo University of Agriculture and Technology, 2-24-16 Naka-cho, Koganei, Tokyo 184-8558, Japan. <sup>5</sup>Research Center for Energy and Environmental Science, Shinshu University, 4-17-1 Wakasato, Nagano 380-8553, Japan. <sup>6</sup>CIRIMAT, Université de Toulouse, CNRS, INPT, UPS, 118 route de Narbonne, 31062 Toulouse Cedex 9, France. <sup>7</sup>Department of Chemistry, University of Cambridge, Lensfield Road, Cambridge CB2 1EW, UK. <sup>8</sup>Department of Materials Science and Engineering, University of California, Los Angeles, California 90095, USA. \*e-mail: [simon@chimie.ups-tlse.fr](mailto:simon@chimie.ups-tlse.fr)

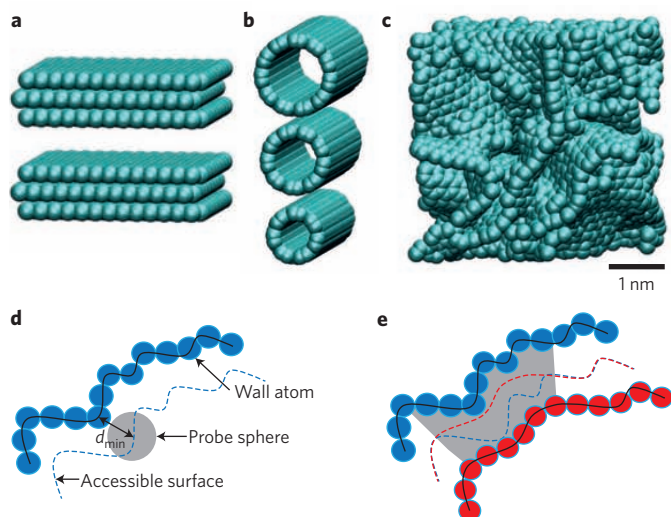


**Figure 1 | Examples of nanoporous carbon structures.** **a-c**, Although ordered structures such as slit pores (**a**) and nanotubes (**b**) exist, most supercapacitors use disordered nanoporous carbons (**c**). The definition of the accessible surface depends on the choice of the probe and on the nature of the porosity. **d,e**, In mesopores, the whole surface is accessible (**d**), whereas in micropores (**e**) some regions of the pores are inaccessible to probe molecules or ions. In **e**, blue and red spheres represent wall atoms at opposite sides of a micropore, and the blue and red dashed lines represent the closest surfaces to these that are accessible by the probe sphere. Where the dashed lines cross, the pore wall is inaccessible, as indicated by the grey-shaded area in **e**.

using the double-layer capacitance model proposed by Helmholtz in 1853 (ref. 10):

$$C = \frac{\epsilon_r \epsilon_0 A}{d} \quad (1)$$

where  $\epsilon_r$  is the electrolyte relative permittivity,  $\epsilon_0$  is the vacuum permittivity,  $d$  is the effective thickness of the double layer (charge separation distance) and  $A$  is the electrode surface area. Note, however, that all these quantities (except for  $\epsilon_0$ ) are ill-defined for the interfaces at play in the present case of highly disordered materials.

Until 2005, it was believed that the best strategy for increasing capacitance consisted in maximizing the electrochemical double-layer charging. The challenge at that time was therefore to develop new mesoporous carbons with the highest specific surface area. Then, following original work from the group of Aurbach<sup>11,12</sup>, the discovery of a different, more efficient storage mechanism in nanopores (pore size less than 1 nm: that is to say, less than the size of solvated ions)<sup>3</sup> led to a change of view: not only the surface area but also the pore size and the carbon nanostructure drive the electrochemical performance. The community thus had to reconsider the way that charge is stored at the carbon/electrolyte interface in ultra-small pores. Since then, much effort has been directed towards the basic understanding of charge storage mechanisms at the nano- and subnanoscales, considering both sides of the interface: the carbon structure and the electrolyte organization, including the (de)solvation of ions and their interactions under extreme confinement.

In this section, we show how the development and the use of new techniques, both theoretical and experimental, have been at the origin of major advances in carbon-based supercapacitors. First, more realistic structural models for porous carbon structures have been developed by coupling modelling and characterization techniques such as small-angle X-ray scattering (SAXS) or neutron scattering (SANS), which greatly improve our understanding of their electrochemical behaviour. In addition, the combination of advanced

electrochemical techniques such as electrochemical quartz crystal microbalance (EQCM), spectroscopies such as nuclear magnetic resonance (NMR) or infrared, and characterization techniques (SAXS), together with modelling, have led to the elucidation of electrolyte organization in carbon nanopores at null potential and under polarization, as well as the charge storage mechanism and the ion dynamics in the pores. These points are detailed below.

**Structural models for nanoporous carbons.** Nanoporous carbons generally consist of defective nanoscale graphitic units, with pores ranging from micropores (pore size <2 nm) to mesopores (from 2 to 50 nm). Unlike slit pores or nanotubes (Fig. 1a,b), they do not display any three-dimensional (3D) long-range ordering (Fig. 1c). Because the electrochemical performance of carbons is driven by the porous carbon/electrolyte interface, accurate and reliable characterizations of the porous network are needed for designing better supercapacitors. Specific surface area and pore size distributions of porous material are generally obtained from gas adsorption techniques, using theoretical models. But such methods suffer from several limitations when applied to microporous carbons.

Choosing an appropriate molecular probe is essential, as pores inaccessible to gas molecules may be accessible to ions from the electrolyte, depending on thermodynamic conditions (Fig. 1d,e). This is specifically true when  $N_2$  adsorption at 77 K is used to measure the carbon specific surface area. The quadrupole moment of the  $N_2$  molecule limits the access of the gas to small micropores, and reduced flexibility of the porous carbon network structures at low temperatures does not necessarily reflect the ambient temperature properties. As a result,  $N_2$  sorption does not give accurate porosity values for ultramicropores (<0.7 nm). Without a quadrupole moment and with a smaller diameter (0.335 nm compared with 0.363 nm), Ar atoms can access small micropores more easily than  $N_2$ . Combined with a higher experimental measurement temperature and a simpler theoretical analysis, this makes Ar adsorption at 87 K more suited than  $N_2$  for the characterization of microporous carbons<sup>13</sup>. A complementary approach involves using the adsorption of supercritical gas or subcritical fluids ( $CO_2$ ) at ambient temperature, which improves the adsorption kinetics.

The choice of the probe and of the experimental conditions is only part of the challenge, as the microscopic features must then be extracted from the experimental isotherm by means of an appropriate model. The Brunauer–Emmett–Teller (BET) analysis<sup>14</sup> is not recommended for microporous carbons, as recently confirmed by the International Union of Pure and Applied Chemistry<sup>15</sup>, as it overestimates the surface of large micropores (>0.7 nm) by 10 to 40%, owing to enhanced bilayer gas adsorption on carbon pore walls. In addition, the BET surface area of ultramicropores (<0.7 nm) is underestimated owing to incomplete monolayer formation. Reliable porosity values for larger micropores (>0.7 nm) can be experimentally obtained by the subtracting pore effect method (SPE) using a high-resolution  $\alpha_s$ -plot, at low relative pressure (from  $P/P_0 = 10^{-6}$ )<sup>16,17</sup>. Moving from measurements of surface area to measurements of pore size distribution, quenched solid density functional theory analysis can provide reasonable structural information from high-resolution adsorption isotherms<sup>18</sup>.

All of this illustrates the difficulty of measuring the surface area of nanoporous carbons. Furthermore, the very concept of 'surface' by itself could be questionable, as it depends on the approach (that is, the probe) used to measure it<sup>19</sup>. Therefore, methods based on molecular probes should be complemented by alternative direct characterization techniques such as SAXS and NMR spectroscopy, which can assess the whole pores of nanoporous carbons that are accessible to the electrolyte ions, and thus are directly relevant to the electrochemical measurement. Despite such limitations, it remains reasonable to discuss the dependence of the capacitance per unit surface area on pore size based on Ar adsorption data, to provide a

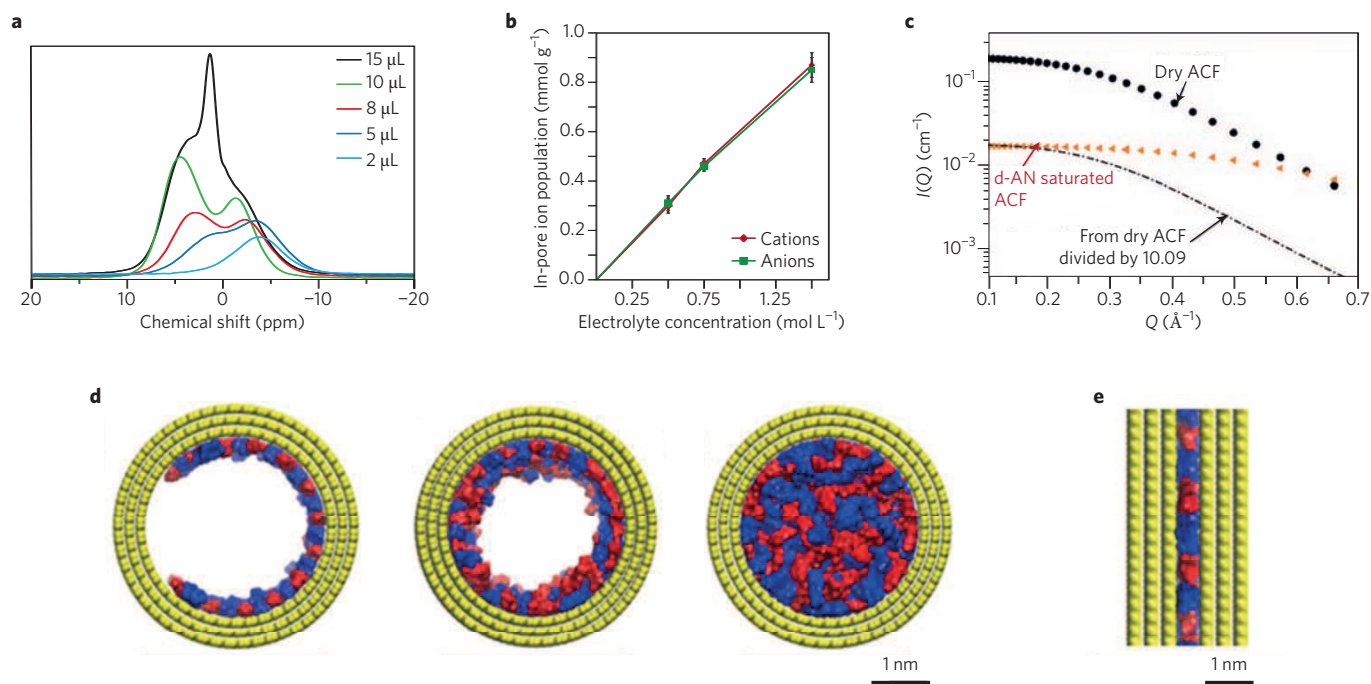


**Figure 2 | Characterization of pore wetting at null potential.** **a**, NMR spectra with different electrolyte loadings inside nanoporous carbon. ppm, parts per million. **b**, Number of ions adsorbed inside the pores with respect to the electrolyte concentration. **c**, Neutron scattering experiments on dry or electrolyte-saturated activated carbon electrodes.  $Q$ , scattering vector;  $I$ , intensity; ACF, activated carbon fabric; AN, acetonitrile. **d,e**, Adsorption of ionic liquids inside a mesopore and a micropore from molecular dynamics simulations (yellow, pore wall atoms; red, cations; blue, anions). Figure reproduced from: **a**, ref. 25, American Chemical Society; **b**, ref. 26, NPG; **c**, ref. 27, American Chemical Society; **d,e**, ref. 28, American Chemical Society.

method for comparison between samples and preparation method. Nevertheless, gravimetric capacitance (farad per gram of carbon) or volumetric capacitance (farad per volume of electrode) is preferred, as these are based on experimental, measured values, free from any theoretical model or structural considerations.

Revealing the ‘real’ structure of nanoporous carbons is much more complex, because it is not currently possible to resolve such structures by resorting only to experimental approaches. To that end, combinations of experimental and modelling techniques have been proposed. One may, for example, use synchrotron X-ray diffraction and SAXS experiments to obtain short- and long-range structural information on the porous carbon network. But scattering techniques usually give access to 1D structural information, and the corresponding data must be transformed into 3D structures by the use of hybrid reverse Monte Carlo simulation<sup>20,21</sup>. Combinations of NMR, pair distribution function analysis of X-ray data, and Raman spectroscopy with lattice simulations have recently been used to evaluate the size of the graphene domains in the porous carbons<sup>22</sup>. Alternatively, quenched molecular dynamics has been used successfully to describe the structure of nanoporous carbons without resorting to experimental structural data<sup>23,24</sup>.

We finally note that most studies so far have focused on the structure of the nanoporous carbon only, whereas the ability to predict the key features of the structure needed to optimize the charge storage also requires a deeper understanding of the structures and dynamics of the confined electrolyte.

**Wetting of the pores at null potential.** Until recently, the charging of supercapacitors was assumed to arise from a simple mechanism of the applied potential driving the ions into the porous carbon network. The first *in situ* NMR studies have shown that this is not the case: even at low electrolyte loadings, NMR signals are observed that are shifted towards lower frequencies, as shown in Fig. 2a (refs 25–29), owing to the aromatic ring-current effects of graphitic domains and magnetic susceptibility of the carbon. The results

indicate that ions (along with the solvent) are adsorbed within the pores. The starting situation at 0 V is therefore better characterized by the interpenetration of the two heterogeneous structures — the solid carbon material and the electrolyte. Molecular dynamics simulations further confirmed this picture, showing that an ionic liquid in contact with a nanoporous carbon electrode spontaneously fills the highly confined nanopores, even without any applied field<sup>30–32</sup>.

NMR spectroscopy is quantitative and thus provides the concentrations of ions adsorbed inside the electrode. The latter follow a linear trend with respect to their counterparts inside the bulk electrolyte<sup>26</sup> (Fig. 2b), thereby confirming the affinity of the ions for the carbon. As the ions diffuse between pores during the signal acquisition, however, they experience various environments, resulting in relatively broad NMR spectra<sup>33</sup>. It is therefore not straightforward to determine the population of the various adsorption sites (for example mesopores versus micropores) using this technique. Another approach is SANS or X-rays. In an empty porous carbon, the signal at small wave vectors originates from the contrast between the carbon atoms and the pore voids. For example, nanopores with a characteristic length scale  $d$  of 1–2 nm display a signature around  $2\pi/d \approx 3–6 \text{ nm}^{-1}$ . When the pores are filled with the electrolyte, this contrast vanishes and the signal decreases. An example of the application of *in situ* SANS to a typical activated carbon, either empty or loaded with an organic electrolyte, is shown in Fig. 2c (ref. 27). The decrease in the scattering intensity depends on the wave vector, revealing an incomplete wetting of the smallest pores.

In contrast, Bañuelos *et al.* combined SANS and molecular dynamics simulations to investigate the adsorption of a room-temperature ionic liquid (RTIL) inside a hierarchical porous carbon at various loadings<sup>28</sup> and concluded that the RTIL covers the pore surfaces uniformly, rather than leaving some pore surfaces unsaturated. Their pictures of the wetting of mesopores and micropores are shown in Fig. 2d and e, respectively. Different results were observed in the case of aqueous electrolytes<sup>34</sup>, suggesting that the surface chemistry of the carbon and the nature of the electrolyte strongly

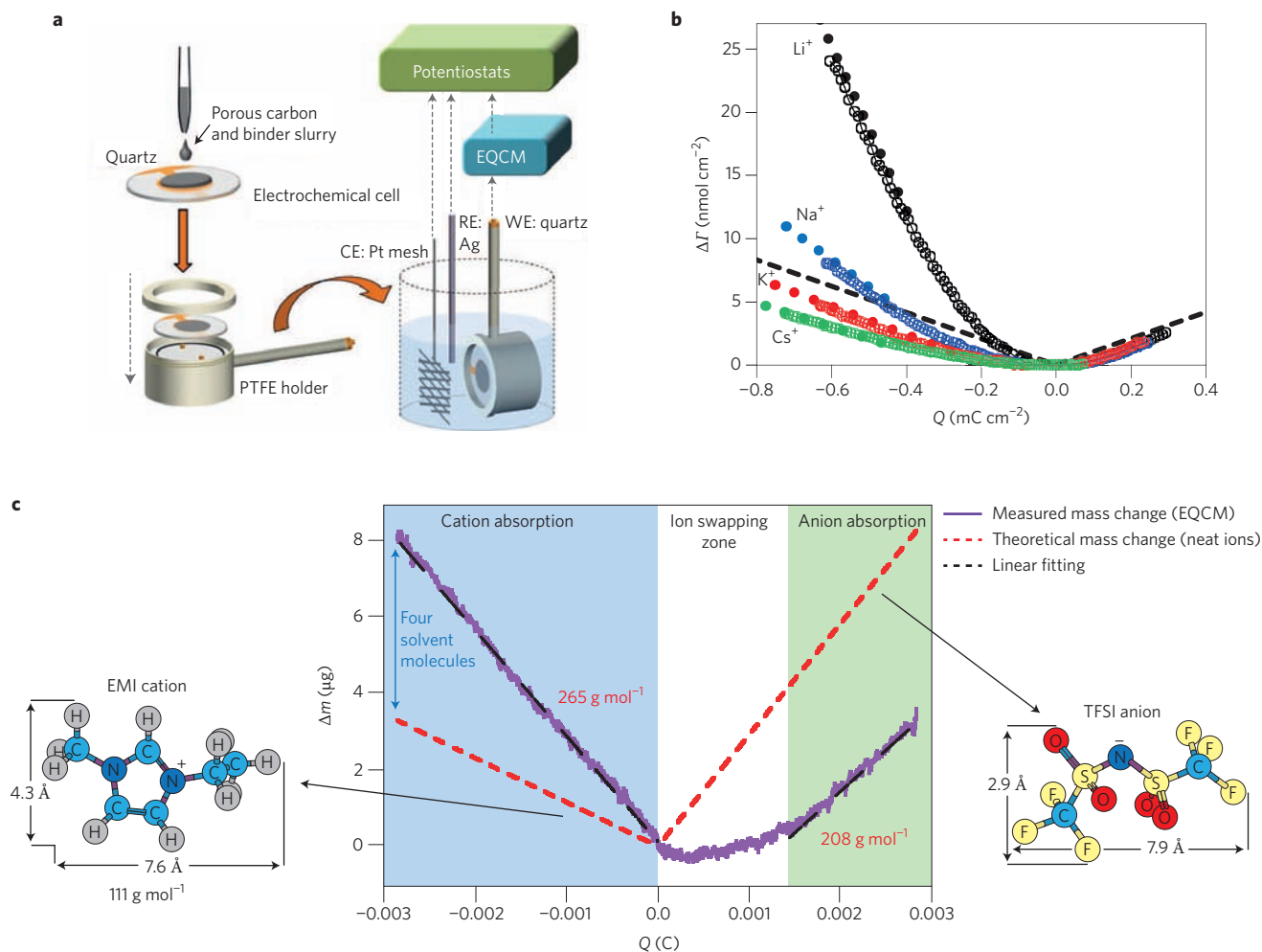


**Figure 3 | Desolvation of the ions in electrified nanopores.** **a**, EQCM set-up. RE, reference electrode; CE, counter electrode; WE, working electrode. **b**, Variation of the adsorption of ions with respect to the accumulated charge per unit area in aqueous electrolytes with various alkali cations. Dashed lines represent the theoretical mass change (Faraday's law for neat ions). **c**, Variation of the mass with respect to the accumulated charge in an organic electrolyte. EMI, 1-ethyl-3-methylimidazolium; TFSI, bis(trifluoromethylsulfonyl)imide anion. Figure reproduced from: **b**, ref. 39, American Chemical Society; **c**, ref. 43, American Chemical Society.

affect the wetting properties. Recently, Kondrat and Kornyshev have proposed to use 'ionophobic' pores for designing a new generation of supercapacitors<sup>35</sup>. Their idea, which remains to be realized experimentally, is built on the fact that such pores would be filled for high voltage only; this could potentially result in larger energy densities and rapid rates of charge and discharge.

**Desolvation in nanopores.** The discovery that ions could access carbon pores smaller than their solvated ion size has revitalized research into ion confinement in carbon nanopores. From electrochemical measurements, it was proposed that ions lose a part of their solvation shell to access these small nanopores (<1 nm). In addition, the capacitance was strongly enhanced when the carbon pore size was in the same range as the ion size<sup>3,36-38</sup>. Although such observations were made using carbon with tailored pore sizes, the use of conventional electrochemical techniques failed to give quantitative information on the extent of desolvation. The development of *in situ* techniques such as EQCM has led to important advances in addressing this issue. Figure 3a shows a schematic of an EQCM set-up; the change of the quartz resonance frequency reflects the change of weight of the active material during the polarization.

The use of EQCM to study ion adsorption in porous carbons was pioneered by Levi and Aurbach<sup>39-41</sup>. Figure 3b shows typical

changes of ion population as a function of the charge accumulated in a porous carbon electrode during polarization in aqueous electrolyte with varying alkali cations<sup>39</sup>. In this example, from the associated mass change and comparison with the theoretical mass change expected for the adsorption of bare ions from Faraday's law, it was shown that the adsorbed Li<sup>+</sup>, Na<sup>+</sup>, K<sup>+</sup> and Cs<sup>+</sup> ions are tightly attached to 2.0, 0.8, 0.1 and 0.0 water molecules on average. The confinement of the ions is therefore accompanied by a substantial decrease in their solvation number (number of solvent molecules around the ion), thus confirming previous results<sup>42</sup>.

EQCM was also used in organic electrolytes in combination with carbons of 1-nm average pore diameter<sup>43</sup>. A solvation number between three and four could be calculated for 1-ethyl-3-methylimidazolium cations confined in the 1-nm pores, much smaller than the eight molecules for cations in the bulk electrolyte. The joint use of NMR spectroscopy and EQCM allowed the effects from the cations and anions to be separated and the cation solvation number to be determined<sup>26</sup>. These results clearly indicate that the partial desolvation of the ions occurs when accessing small pores. The decrease in the ion solvation number could also be quantified directly in molecular dynamics simulations<sup>31</sup>. Importantly, these studies point out a difference in the energy storage mechanism depending on the electrode polarity, as described below in more detail.

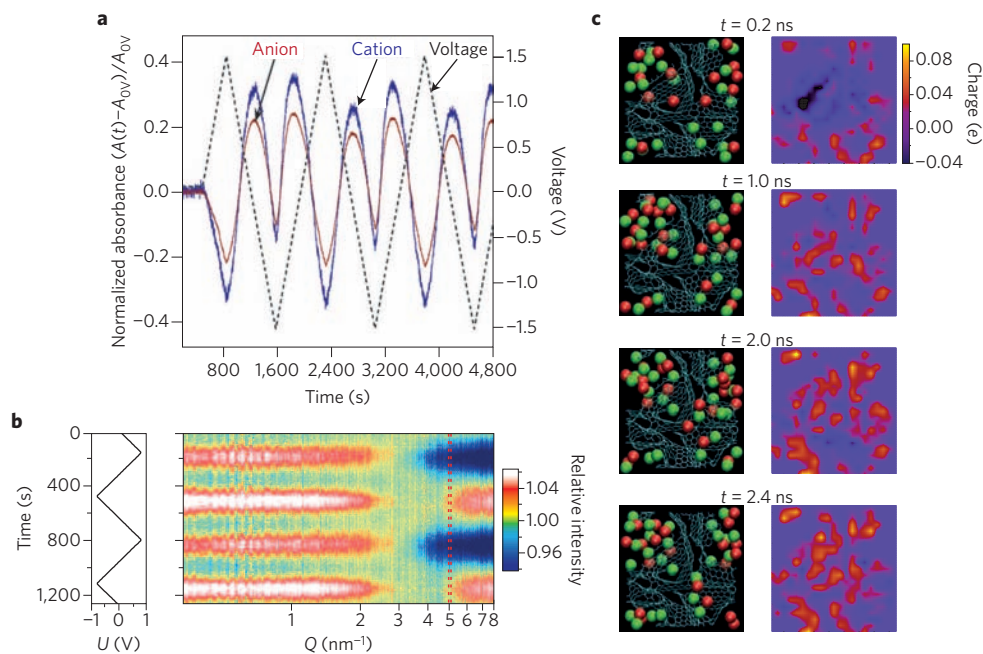


**Figure 4 | Characterization of the charging dynamics of supercapacitors.** **a**, Temporal variation of the normalized infrared absorbance for various charge–discharge cycles (ionic liquid electrolyte). **b**, Temporal variation of the SAXS intensity (right panel) for various charge–discharge cycles (aqueous CsCl electrolyte).  $Q$ , scattering vector. The evolution of the applied potential  $U$  with time is shown in the left panel. **c**, Time evolution of the local charge on the carbon atoms on charging in a molecular dynamics simulation (turquoise sticks, C–C bonds; red spheres, cations; green spheres, anions). Figure reproduced from: **a**, ref. 60, American Chemical Society; **b**, ref. 61, RSC; **c**, ref. 65, American Chemical Society.

**Charge storage mechanism.** Although the basic principle underlying charge storage in EDLCs, namely the adsorption of ions at the surface of the electrode, is well established, the corresponding microscopic mechanisms have remained elusive until recently. The Gouy–Chapman–Stern theory, which has been the cornerstone of theoretical electrochemistry for over a century, predicts that near an extended surface, the electrode charge is balanced by the polarization of the electrolyte. The decay of the ionic charge distribution and of the electrostatic potential occurs over the ‘Debye length’, typically in the 1–10 nm range, which depends on the electrolyte concentration and solvent permittivity. But this picture is of limited help in understanding the interfacial structure and thermodynamics in the case of supercapacitors, owing to the strong ionic correlations at high electrolyte concentration or in pure ionic liquids<sup>44</sup> and to the marked effects of confinement<sup>30–32,45</sup>. The behaviour of such electrolytes near metallic walls, noticed as early as 1952<sup>46</sup>, has called for a paradigm change<sup>44,47</sup>, and recent advances in simulation techniques<sup>48</sup> have shown that it is also important to consider the electrolyte structure at the electrode surface<sup>49,50</sup>. Recent claims based on surface force apparatus experiments have also revived the debate on the differences between electrochemical interfaces involving pure ionic liquids and those of solvent-based electrolytes<sup>51–54</sup>.

In the case of planar graphitic electrodes, the Gouy–Chapman–Stern theory predicts an increase in the capacitance with the applied potential. This theory does not, however, capture two important features, namely the ionic correlations and the finite surface area accessible to the ions. This explains why it fails at reproducing, even qualitatively, experimental results in highly concentrated electrolytes<sup>47</sup>. Mean-field theories accounting for these effects and molecular simulations<sup>44,55</sup> show that the differential capacitances may display various shapes (the ‘camel’ or ‘bell’ shapes) depending on the nature of the electrolyte. But these capacitance values remain too small to be exploited efficiently in supercapacitor devices.

An important consideration for extreme confinement, when pore sizes are comparable to the diameter of the ions, is that the electronic charge inside the electrode is compensated by an imbalance in the

number of co- and counter-ions inside the pores. In such a ‘super-ionic state’, the local breakdown of electro-neutrality in the interstitial fluid is compensated by the creation of a corresponding charge on the metallic surface that efficiently screens the interactions between like-charged ions<sup>56,57</sup>. Several processes may lead to the overall excess of counter-ions inside an electrode: adsorption of counter-ions, swapping of co-ions for counter-ions, or desorption of co-ions<sup>58</sup>. For a given combination of electrodes and electrolyte (nature of the ions, presence and choice of a solvent), one or several of these mechanisms are observed as a function of voltage. NMR, molecular dynamics, infrared spectroscopy, SAXS and EQCM suggest that ion swapping is the most common process at low voltage, but for large ion sizes and/or at high voltage, adsorption of the sole counter-ions is also observed, as illustrated in Fig. 3c. Desorption of co-ions seems to be less frequent. Recent *in situ* NMR measurements on a solvent-based electrolyte have shown that the charge storage mechanism can differ depending on the electrode polarization; ion swapping was observed for positive polarization, whereas counter-ion adsorption dominated for negative polarization. This suggests that multiple factors may influence how excess ionic charge is achieved, including relative sizes and mobilities of co/counter-ions, kinetic phenomena and ion rearrangement over multiple cycles. Coupling NMR with EQCM also showed that both counter-ion adsorption and ion swapping are accompanied by the entrance or departure of solvent molecules<sup>26</sup>. In pure ionic liquids, molecular simulations suggest that the exchange occurs almost without changing the volume occupied by the liquid inside the electrode<sup>30</sup>, but this conclusion should be strengthened by considering further combinations of cations and anions, and requires experimental confirmation.

The fundamental understanding of the microscopic charging mechanisms achieved in the past five years provides a strong basis for the design of better supercapacitors, by suggesting new strategies for the optimization of charge storage through appropriate combinations of electrode structures, ions and solvent. The widespread use of experimental and simulation tools developed to establish these mechanisms will be the key to the success of this endeavour.

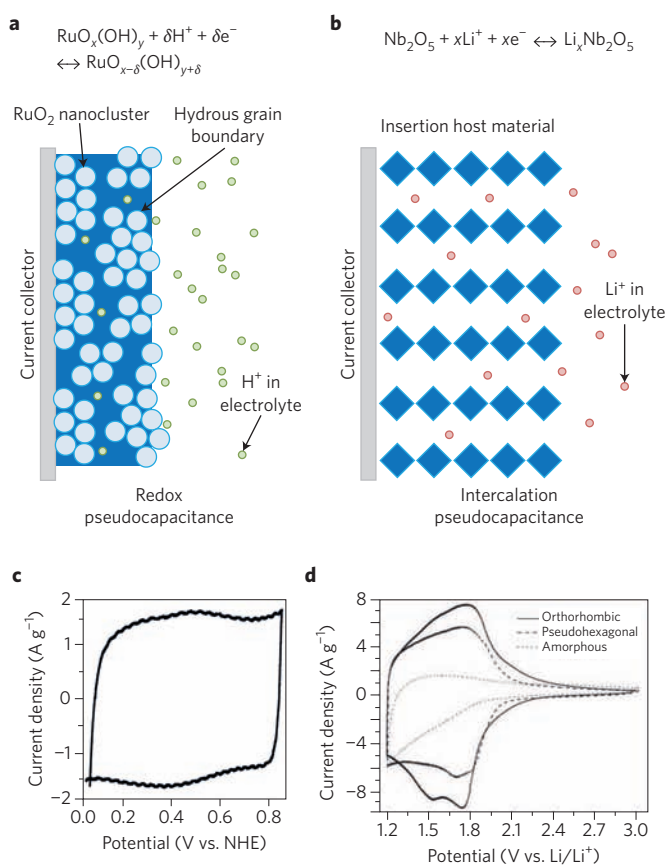


**Figure 5 | Different types of pseudocapacitive behaviour.**

**a**, Redox pseudocapacitance in  $\text{RuO}_2$  occurs in the near-surface region. **b**, Intercalation pseudocapacitance in  $\text{Nb}_2\text{O}_5$  (T-phase) is a bulk effect from  $\text{Li}^+$  insertion. **c**, Cyclic voltammetry experiments show the  $\text{RuO}_2$  to have the traditional capacitor 'box'. **d**, Cyclic voltammetry experiments show that the orthorhombic  $\text{Nb}_2\text{O}_5$  (T-phase) exhibits redox peaks with little voltage offset. Figure reproduced from: **a, b**, ref. 66, RSC; **c**, ref. 69, American Chemical Society; **d**, ref. 67, Wiley.

**Dynamics of charging and discharging.** The key feature of supercapacitors, for example with respect to batteries, is their very high power density: they are able to charge or discharge within a few seconds. The increase in capacitance should therefore not be achieved at the price of a decrease in power. Conventional theories predict that liquids suffer from noticeable slowdown of their dynamics when they are strongly confined, disqualifying in principle the use of microporous carbons for supercapacitors. Fortunately, such effects have not been observed in experiments performed on carbide-derived carbons (CDCs), for which a maximal characteristic discharge time of 20 seconds was obtained for the smallest average pore size<sup>3</sup>. This trend is further confirmed by electrochemical impedance spectroscopy. This technique offers the possibility of measuring in-pore resistivities in the low-frequency region. These resistivities are usually of the order of 50 to 200 ohm cm for electrolytes made of organic ions dissolved in acetonitrile at room temperature — only slightly higher than for the same liquids under bulk conditions<sup>59</sup>.

The fast charging of supercapacitors impedes the application of the usual *in situ* techniques to monitor their dynamical behaviour. In many cases, the time needed to record a spectrum or a diffractogram is longer than their charging time. However, techniques such as infrared spectroscopy or SAXS have been used to study charge/discharge cycles of supercapacitors at a low scan rate of  $5 \text{ mV s}^{-1}$ . Figure 4a and b shows the relative evolution of the signal with time and potential, in two different experiments. In one case, a supercapacitor made of

1-ethyl-3-methylimidazolium bis(trifluoromethylsulfonyl)imide ionic liquid and a CDC electrode is studied by infrared spectroscopy<sup>60</sup>. In the second case, the adsorption of an aqueous CsCl electrolyte inside a microporous activated carbon is studied by SAXS<sup>61</sup>. In both cases, the response of the liquid closely follows the applied potential, with a lag of only a few seconds. These observations are consistent with a timescale of seconds for charging microporous supercapacitors. NMR and magnetic resonance imaging (MRI) studies have highlighted the role of the cell design in the timescale of ionic response during charging. Using a non-optimal 'shifted' cell design to allow electrodes to be studied independently, *in situ* NMR experiments revealed a lag between the applied potential and charge build up on the electrode even at a low scan rate, which is due to ohmic drop<sup>25</sup>. This issue was subsequently addressed through the use of MRI which allows spatial resolution of the two electrodes in a conventional cell design<sup>62</sup>.

The microscopic origin of the observed fast charging has been studied using molecular simulations. In particular, molecular dynamics provides the trajectories of the molecules and is perfectly suited for extracting transport properties such as diffusion coefficients. Recent work has shown that the diffusion coefficients of the ions are generally one to two orders of magnitude smaller in the electrodes than in the bulk liquid<sup>59,63</sup>, but strong variations are observed with the filling of the electrode in the case of ionic liquids<sup>63,64</sup>. Indeed, Kondrat *et al.* have shown that in slit pores, the ions can even diffuse faster than in the bulk at intermediate voltages<sup>63</sup>. In CDCs, this effect is not observed but the good connectivity between the pores was shown to be an important characteristic, allowing the larger pores to play the role of electrolyte reservoirs as shown in Fig. 4c (ref. 65). Injecting molecular dynamics results into an equivalent circuit model then leads to estimated charging times of 1 to 10 s for CDC electrodes<sup>65</sup>, further demonstrating the good predictive power of these simulations.

### Oxide-based supercapacitors

In the 1970s, Conway and others recognized that certain materials undergo redox reactions at or near their surface and yet their electrochemical properties are similar to those of supercapacitors, which store energy at the electrical double layer formed at the electrode/electrolyte interface<sup>1</sup>. These pseudocapacitive materials lead to much higher levels of charge storage than EDLCs, owing to the redox reactions<sup>4</sup>. For this reason, over the past several years there has been growing interest in pseudocapacitors because of the prospect of achieving the high energy density of traditional battery electrode materials combined with the long cycle life and power density of EDLCs<sup>66</sup>.

**The mechanism of pseudocapacitance.** The most widely investigated pseudocapacitors are  $\text{RuO}_2$  and  $\text{MnO}_2$ . As the field has developed, certain metrics have emerged that provide a more rigorous identification of pseudocapacitance. In particular, materials exhibiting high energy density at high discharge/charge rates display electrochemical signatures that are representative of pseudocapacitive behaviour. An especially good model system in which to characterize pseudocapacitance is  $\text{Nb}_2\text{O}_5$ , as 70% of its theoretical capacity for lithium can be stored in only 1 minute ( $125 \text{ mAh g}^{-1}$  for 1-minute discharge)<sup>67</sup>. Moreover, charge storage by means of redox reactions takes place in the bulk of the material and not only at the surface as is commonly thought<sup>68</sup>. The charge storage mechanism involved here, intercalation pseudocapacitance, is not controlled by semi-infinite diffusion and instead exhibits the fast kinetic response observed in double-layer capacitors (leading to high power) despite the fact that charge storage arises from redox reactions. A comparison between intercalation pseudocapacitance and the redox pseudocapacitance<sup>69</sup> that characterizes  $\text{RuO}_2$  is shown in Fig. 5. Some of the key electrochemical responses associated with pseudocapacitance include: (i) a linear dependence of the potential on the state of charge; (ii) a charge-storage capacity mostly independent of rate; and (iii) redox



peaks with small voltage offsets<sup>70</sup>. Materials that do not show such features should not be considered pseudocapacitive. The recent paper by Brousse *et al.* points out the limitations in describing materials such as Ni(OH)<sub>2</sub> or cobalt oxides as being pseudocapacitive<sup>71</sup>.

**Pseudo-intercalation reactions.** Another important consideration for pseudocapacitive materials is that the structure does not undergo a phase transformation on intercalation. In this regard, when MoO<sub>2</sub> is prepared as a nanoscale material, its characteristic monoclinic-to-orthorhombic phase transition, which occurs on lithiation, is suppressed and the material shows the pseudocapacitive responses mentioned above. The gravimetric capacity for nanoscale MoO<sub>2</sub> for 2-minute discharge rate is nearly 200 mAh g<sup>-1</sup>, far exceeding the energy density of any other material at this rate<sup>72</sup>. Additional studies show that pseudocapacitive behaviour is preserved even in 40- $\mu$ m-thick Nb<sub>2</sub>O<sub>5</sub> films. Such films have been incorporated in a hybrid cell comprising a Nb<sub>2</sub>O<sub>5</sub> negative electrode and activated carbon as the positive electrode<sup>68</sup>. Although this device showed very good performance, it was limited by the energy density of the carbon electrode, which stores energy by means of the electrical double layer.

One of the more popular approaches to developing pseudo-capacitor materials involves the synthesis of nanoscale materials<sup>73</sup>. Growing evidence indicates that electrochemical characteristics tend to become more capacitor-like when the crystallite is smaller than 20 nm. For example, the potential dependence on state of charge (see (i) above) can become linear owing to a larger number of surface sites for charge storage or the suppression of a phase transition. Kinetics are also influenced by the small crystallite size, as the decrease in diffusion distance leads to higher power density. In addition, the use of sweep voltammetry to separate diffusion-controlled kinetics from capacitive processes shows nanoscale materials to be more capacitor-like<sup>66</sup>. Thus far, the charge storage mechanisms for only a few 2D materials prepared in the form of nanosheets have been characterized. In the case of TiO<sub>2</sub>, a surface-controlled response reported for this material is expected, as nearly the entire surface of the sample is exposed to electrolyte<sup>74</sup>.

To account for the role of nanostructuring, Simon, Dunn and colleagues recently proposed that pseudocapacitance can be intrinsic or extrinsic to a material<sup>68</sup>. An intrinsic pseudocapacitor shows the various electrochemical signatures of double-layer capacitors regardless of particle size or shape: MnO<sub>2</sub> is a good example of intrinsic behaviour<sup>71,75,76</sup>, although the structural behaviour and charge storage of the material changes from one allotrope to another<sup>77</sup>, as shown by *in situ* synchrotron X-ray diffraction analyses<sup>78</sup>. In contrast, the extrinsic term applies to materials that show pseudocapacitor characteristics only as nanoparticles. With these materials, the diffusion distance is less than  $(Dt)^{1/2}$ , where  $D$  is the diffusion coefficient and  $t$  the time. These materials do not show pseudocapacitive behaviour in the bulk state. The extent to which nanostructuring produces pseudocapacitance is likely to cover a wide range of transition metal oxides, sulfides and nitrides, and is currently an active area of research. As shown with MoO<sub>2</sub>, the extrinsic pseudocapacitor approach provides the exciting opportunity of creating materials that possess both the high energy density of battery materials and the high power density of capacitors.

### Hybrid supercapacitors

The desire to increase the energy density of EDLCs coupled with the growing interest in pseudocapacitor materials has led to the design of composite hybrid materials<sup>79,80</sup>. The development of these fast charge/discharge materials is providing the basis for creating the next generation of hybrid supercapacitors.

The most advanced hybrid supercapacitors are based on the use of high-rate Li<sub>4</sub>Ti<sub>5</sub>O<sub>12</sub> (LTO), another lithium-ion insertion material. This material retains a lithium capacity in excess of 120 mAh g<sup>-1</sup> at a charge/discharge rate of 30C (full discharge in 2 min). Moreover,

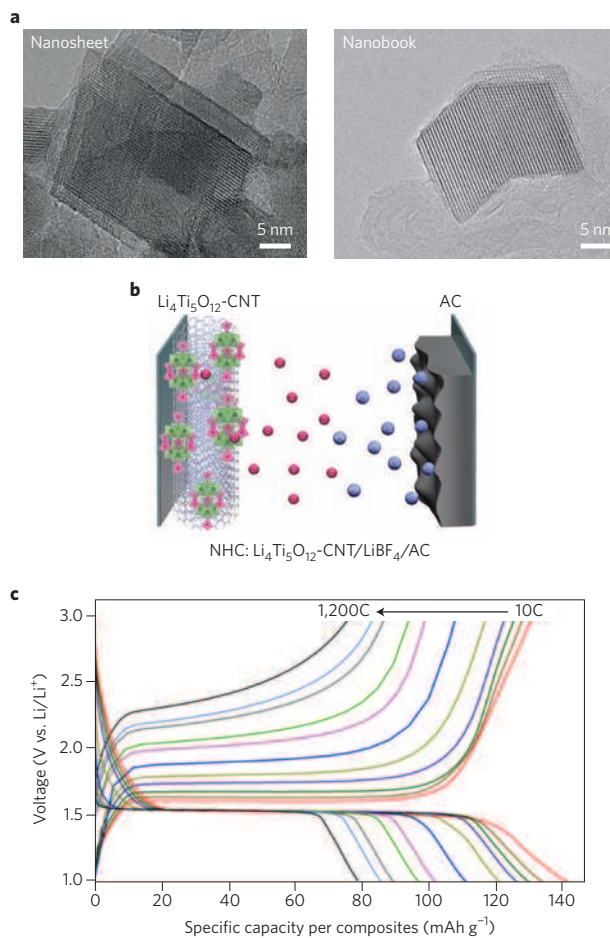


**Figure 6 | Nano hybrid supercapacitor set-up and characterization.**

**a**, High-resolution transmission electron microscope images of nanocrystalline Li<sub>4</sub>Ti<sub>5</sub>O<sub>12</sub> prepared as 'nanosheets' and/or 'nanobooks' that are fabricated in composites with CNTs using ultracentrifugation (~75,000g). **b**, Nano hybrid capacitor (NHC) using an activated carbon (AC) and dimension-controlled Li<sub>4</sub>Ti<sub>5</sub>O<sub>12</sub> nanocrystals composited with single-walled CNTs. **c**, Discharge curves at various C-rates (from 10 to 1,200) after charging at a fixed rate of 10C. Figure reproduced from: **a,c**, ref. 85, American Chemical Society; **b**, ref. 84, RSC.

in contrast to MnO<sub>2</sub> and RuO<sub>2</sub> which operate in aqueous electrolytes within a limited potential window (about 1 V), LTO functions in high-voltage non-aqueous electrolytes. LTO cannot be defined as a pseudo-capacitive material, as it shows a voltage plateau and undergoes a phase change during lithiation. Because it exhibits zero strain and supports rapid Li<sup>+</sup> ion transport during the (de)intercalation reaction, however, LTO is suitable for use in high-rate electrodes in hybrid supercapacitors, devices that combine a faradaic battery electrode with a capacitive electrode. The first generation of commercial hybrid supercapacitors, called the Li-ion capacitor, was based on combining a negative graphite electrode of a Li-ion battery with a capacitive porous-carbon positive electrode<sup>81</sup>. The use of ultrafast Li-ion intercalation materials such as LTO could greatly increase the power capability of such devices, while preserving high energy density<sup>82</sup>.

In recent work, ultracentrifugation synthesis has been explored to further extend the performance of high-rate and pseudocapacitive materials such as RuO<sub>2</sub> (ref. 83). The ultracentrifugation process enables the preparation of nano-sized, dimension-controlled (1D to 2D) materials, directly bound on high-surface-area carbons such as carbon nanotubes (CNT) or disordered porous carbons<sup>84</sup>. Dimension-controlled 2D-LTO is shown in Fig. 6a. High-resolution

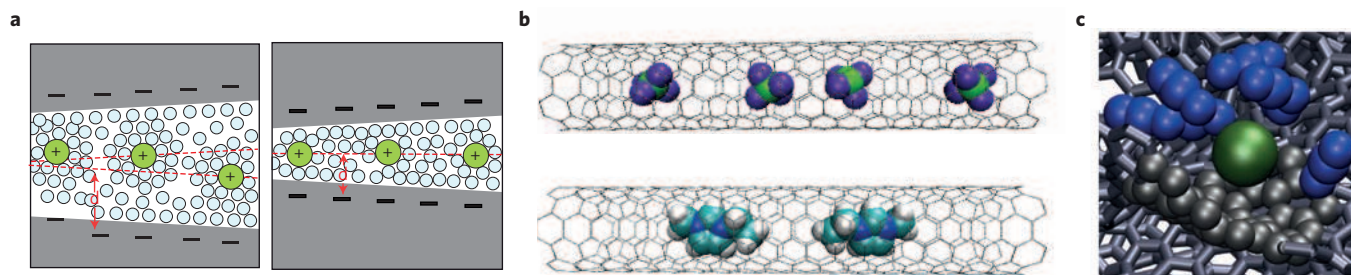


**Figure 7 | Evolution of the picture of the electrode/electrolyte interface in the past decade.** **a**, Ions (green spheres) surrounded by solvent molecules (blue spheres) residing in pores with size between 1 and 2 nm (left), and less than 1 nm (right), as pictured in 2006. **b**, Adsorption of  $\text{BF}_4^-$  anions (top) and 1-ethyl-3-methylimidazolium cations (bottom) inside carbon nanotubes that are positively or negatively charged, as seen in 2010 (green, B; violet, F; turquoise, C; blue, N; white, H; black sticks, C-C bonds of the nanotubes). **c**, Adsorption of partially desolvated  $\text{PF}_6^-$  ion in a disordered nanoporous carbon, as simulated in 2013 (green,  $\text{PF}_6^-$ ; blue, acetonitrile molecules; black, C atoms in contact with the anion; black sticks, C-C bonds of the electrode). Figure reproduced from: **a**, ref. 3, AAAS; **b**, ref. 32, American Chemical Society; **c**, ref. 31, NPG.

transmission electron microscopy images clearly demonstrate that 2D-LTO nanosheets nucleate from the CNT surface and are firmly attached to it. Fast Fourier transform analysis revealed the  $d$ -spacing of lattice fringes as 4.81 Å, corresponding to the (111) plane of the 3D spinel structure<sup>85</sup>. The surrounding interstitial carbon influences the growth direction, shape and size of the 2D-LTO crystals. One fascinating nanoscale morphology is that which occurs from two interconnected LTO nanosheets (a ‘nanobook’; Fig. 6a). These dimension-controlled LTO show ultrafast charge/discharge behaviour when operated in excess of 300C (full discharge in 12 s) and as high as 1,200C (full discharge in 3 s), as shown in Fig. 6c.

Energy storage devices based on hybrid supercapacitors are being commercialized, and this underscores the importance of these new materials. A three- to fivefold increase in energy density compared with conventional carbon-based EDLCs has been achieved by combining a negative electrode made of ultracentrifugation-prepared LTO nanosheets with a porous-carbon positive electrode. Although the stability of the nanostructured electrode/electrolyte interfaces is still an important issue to be solved, this technology has the potential to become an alternative to EDLCs<sup>84</sup>.

## Outlook

Supercapacitor electrodes, which used to be a black box, can now be probed at the molecular scale using a variety of experimental and simulation techniques. Our view on the structure of the interface has profoundly changed in the past ten years, as summarized in Fig. 7. The discovery of a new storage mechanism inside nanoporous carbons has enabled large improvements in the energy density of commercial EDLC devices, which now reach specific energies beyond 6–7 Wh kg<sup>-1</sup>. These devices are now used in power electronics, in cars (stop/start systems), and in public transport systems such as trams and buses. The next challenge will be to push this limit further (>10 Wh kg<sup>-1</sup>), thus establishing supercapacitors as ideal candidates in other key applications.

If we consider only porous carbon-based supercapacitors, the possibilities are virtually infinite. On the electrode side of the interface, it is possible to tune the carbon porosity, composition (by activation or using dopants) and microstructure<sup>86</sup>. The impact of carbon doping remains to be understood. For example, including nitrogen in the structure enhances the performance thanks to an additional faradaic contribution, so far limited to aqueous electrolytes<sup>87</sup>. On the electrolyte side, numerous cations, anions and solvent molecules can be used. The development of high-throughput techniques, such as the ones already applied to battery materials and electrolytes<sup>88</sup>, will be a big step forward in that direction<sup>89</sup>. But there is still a need for systematically defining the good descriptors that can be extracted from simulations in order to select a few promising systems among thousands of candidates. Clearly such descriptors can only be designed

from the knowledge gained from the combination of all the information extracted from *in situ* experiments and understanding at the molecular level. Once the relationships among the carbon morphology, the pore size distribution, the size of the ions and the capacitance of the systems are established, the key for enhanced energy densities will depend on surface functionalization<sup>90</sup> and on improvement of the operating potential by formulating better electrolytes<sup>91,92</sup>.

The potential for improvement is even larger for oxide-based pseudocapacitors. Although recent studies have shed some light on the main features of the various mechanisms involved (for example simple surface redox reactions versus pseudo-intercalation), their molecular aspects remain mostly unknown. There is, therefore, an explicit need to adapt the *in situ* experiments and simulations that have been successfully applied to carbon-based supercapacitors for oxide materials. But there are challenges due to the difficulty in obtaining well-defined interfaces both structurally and chemically. Certain oxide supercapacitors operate in aqueous solvents for which acid/base effects must be taken into account, whereas other oxide systems involve the development of nanostructured, nanocrystalline metal oxide particles operating in non-aqueous electrolyte. Two-dimensional materials such as MoS<sub>2</sub> and the compounds known as MXenes have recently been tested for supercapacitor applications<sup>93,94</sup>. Here also, pseudocapacitive effects are at play, but it is likely that the microscopic mechanisms derived for oxide materials will not be relevant for these materials. The use of *in situ* characterization techniques<sup>95,96</sup> will be a decisive step towards improving the energy density of these materials.

Fundamental understanding of ion adsorption and charge storage in supercapacitors is essential for applications and technologies. In the area of energy storage, adsorption processes in porous carbons are of central importance for several technologies. One noteworthy example is redox flow batteries<sup>97</sup>, both aqueous and non-aqueous, which are rapidly progressing towards commercialization because of both centralized and distributed systems that store energy from renewable sources. Biofuel cells, both enzymatic and microbial, represent a well-established sustainable technology in which adsorption processes on porous carbon electrodes are critical for achieving the redox processes involved in energy conversion<sup>98</sup>. Other emerging energy technologies include flow capacitors<sup>99</sup> and ‘blue energy’. The latter is based on extracting the energy associated with the mixing of fresh river and salty seawater<sup>100</sup> or on osmotic power harvesting under salinity gradients<sup>101</sup>. In addition, applications of ion adsorption in carbon-based systems extend beyond energy storage to areas such as biosensors<sup>102</sup> as well as gas-phase sensors for detection of toxic gases<sup>103</sup>, while the use of carbon electrodes for desalination represents an increasingly attractive technology for drought-stricken areas. As these examples show, the experimental and theoretical tools developed and the knowledge gained for supercapacitors provide the basis for the development of a wide range of current and future technologies.

## References

1. Conway, B. E. *Electrochemical Supercapacitors: Scientific Fundamentals and Technological Applications* (Springer, 1999).
2. Miller, J. R. & Simon, P. Electrochemical capacitors for energy management. *Science* **321**, 651–652 (2008).
3. Chmiola, J. *et al.* Anomalous increase in carbon capacitance at pore sizes less than 1 nanometer. *Science* **313**, 1760–1763 (2006).  
**This paper demonstrates that microporous carbons can be used to maximize the capacitance, owing to the desolvation of the ions in subnanometre pores.**
4. Toupin, M., Brousse, T. & Bélanger, D. Charge storage mechanism of MnO<sub>2</sub> electrode used in aqueous electrochemical capacitor. *Chem. Mater.* **16**, 3184–3190 (2004).  
**This paper shows that MnO<sub>2</sub>-based supercapacitors can achieve very high specific capacitances, highlighting the importance of pseudocapacitive mechanisms.**
5. Simon, P. & Gogotsi, Y. Materials for electrochemical capacitors. *Nature Mater.* **7**, 845–854 (2008).
6. Béguin, F., Presser, V., Balducci, A. & Frackowiak, E. Carbons and electrolytes for advanced supercapacitors. *Adv. Mater.* **26**, 2219–2251 (2014).
7. Raccichini, R., Varzi, A., Passerini, S. & Scrosati, B. The role of graphene for electrochemical energy storage. *Nature Mater.* **14**, 271–279 (2015).
8. Armand, M., Endres, E., MacFarlane, D. R., Ohno, H. & Scrosati, B. Ionic-liquid materials for the electrochemical challenges of the future. *Nature Mater.* **8**, 621–629 (2009).
9. Brandt, A., Pohlmann, S., Varzi, A., Balducci, A. & Passerini, S. Ionic liquids in supercapacitors. *MRS Bull.* **38**, 554–559 (2013).
10. Helmholtz, H. Ueber einige Gesetze der Vertheilung elektrischer Ströme in körperlichen Leitern mit Anwendung auf die thierisch-elektrischen Versuche. *Ann. Phys. Chem.* **165**, 211–233 (1853).
11. Eliad, L., Salitra, G., Soffer, A. & Aurbach, D. Ion sieving effects in the electrical double layer of porous carbon electrodes: estimating effective ion size in electrolytic solutions. *J. Phys. Chem. B* **105**, 6880–6887 (2001).
12. Eliad, L., Salitra, G., Soffer, A. & Aurbach, D. On the mechanism of selective electroadsorption in the pores of carbon molecular sieves. *Langmuir* **21**, 3198–3202 (2005).
13. Wang, S., Minami, D. & Kaneko, K. Comparative pore structural analysis of highly porous graphene monoliths treated at different temperatures with adsorption of N<sub>2</sub> at 77.4 K and of Ar at 87.3 K and 77.4 K. *Micropor. Mesopor. Mater.* **209**, 72–78 (2015).
14. Brunauer, S., Emmett, P. H. & Teller, E. Adsorption of gases in multimolecular layers. *J. Am. Chem. Soc.* **60**, 309–319 (1938).
15. Thommes, M. *et al.* Physisorption of gases, with special reference to the evaluation of surface area and pore size distribution. *Pure Appl. Chem.* **87**, 1051–1069 (2015).
16. Kaneko, K., Ishii, C., Ruike, M. & Kuwabara, H. Origin of superhigh microcrystalline graphitic structures of activated carbons. *Carbon* **30**, 1075–1088 (1992).
17. Setoyama, N., Suzuki, T. & Kaneko, K. Simulation study on the relationship between a high resolution  $\alpha$ -plot and the pore size distribution for activated carbon. *Carbon* **36**, 1459–1467 (1998).
18. Neimark, A. V., Lin, Y., Ravikovitch, P. I. & Thommes, M. Quenched solid density functional theory and pore size analysis of micro-mesoporous carbons. *Carbon* **47**, 1617–1628 (2009).  
**This paper provides the theoretical basis of density functional theory, which is now the most used method for characterizing the surface area of microporous carbons.**
19. Centeno, T. A., Sereda, O. & Stoeckli, F. Capacitance in carbon pores of 0.7 to 15 nm: a regular pattern. *Phys. Chem. Chem. Phys.* **13**, 12403–12406 (2011).
20. Bandosz, T. J. *et al.* in *Chemistry and Physics of Carbon* 41–228 (Marcel Dekker, 2001).
21. Bousige, C. *et al.* Realistic molecular model of kerogen's nanostructure. *Nature Mater.* **15**, 576–582 (2016).
22. Forse, A. C. *et al.* New insights into the structure of nanoporous carbons from NMR, Raman, and pair distribution function analysis. *Chem. Mater.* **27**, 6848–6857 (2015).
23. Palmer, J. C. *et al.* Modeling the structural evolution of carbide-derived carbons using quenched molecular dynamics. *Carbon* **48**, 1116–1123 (2010).
24. Palmer, J. C. & Gubbins, K. E. Atomistic models for disordered nanoporous carbons using reactive force fields. *Micropor. Mesopor. Mater.* **154**, 24–37 (2012).
25. Wang, H. *et al.* Real-time NMR studies of electrochemical double-layer capacitors. *J. Am. Chem. Soc.* **133**, 19270–19273 (2011).
26. Griffin, J. M. *et al.* *In situ* NMR and electrochemical quartz crystal microbalance techniques reveal the structure of the electrical double layer in supercapacitors. *Nature Mater.* **14**, 812–819 (2015).  
**This paper shows, by combining *in situ* electrochemical and spectroscopy techniques, that different ion adsorption mechanisms can dominate the charging process of supercapacitors depending on the polarization of the electrode.**
27. Boukhalifa, S. *et al.* *In-situ* small angle neutron scattering revealing ion sorption in microporous carbon electrical double layer capacitors. *ACS Nano* **8**, 2495–2503 (2014).
28. Bañuelos, J. L. *et al.* Densification of ionic liquid molecules within a hierarchical nanoporous carbon structure revealed by small angle scattering and molecular dynamics simulation. *Chem. Mater.* **26**, 1144–1153 (2014).
29. Deschamps, M. *et al.* Exploring electrolyte organization in supercapacitor electrodes with solid-state NMR. *Nature Mater.* **12**, 351–358 (2013).
30. Merlet, C. *et al.* On the molecular origin of supercapacitance in nanoporous carbon electrodes. *Nature Mater.* **11**, 306–310 (2012).  
**This paper provides the first quantitative picture of the structure of an ionic liquid adsorbed inside realistically modelled microporous carbon electrodes.**
31. Merlet, C. *et al.* Highly confined ions store charge more efficiently in supercapacitors. *Nature Commun.* **4**, 2701 (2013).
32. Shim, T. & Kim, H. J. Nanoporous carbon supercapacitors in an ionic liquid: a computer simulation study. *ACS Nano* **4**, 2345–2355 (2010).
33. Merlet, C., Forse, A. C., Griffin, J., Frenkel, D. & Grey, C. P. Lattice simulation method to model diffusion and NMR spectra in porous materials. *J. Chem. Phys.* **142**, 094701 (2015).
34. Boukhalifa, S., He, L., Melnichenko, Y. B. & Yushin, G. Small-angle neutron scattering for *in situ* probing of ion adsorption inside micropores. *Angew. Chem. Int. Ed.* **52**, 4618–4622 (2013).
35. Kondrat, S. & Kornyshev, A. Pressing a spring: what does it take to maximize the energy storage in nanoporous supercapacitors? *Nanoscale Horiz.* **1**, 45–52 (2016).
36. Largeot, C. *et al.* Relation between the ion size and pore size for an electric double-layer capacitor. *J. Am. Chem. Soc.* **130**, 2730–2731 (2008).
37. Galhena, D. T., Bayer, B. C., Hofmann, S. & Amarantunga, G. A. Understanding capacitance variation in sub-nanometer pores by *in situ* tuning of interlayer constrictions. *ACS Nano* **10**, 747–754 (2016).
38. Raymundo-Pinero, E., Kierzek, K., Machnikowski, J. & Béguin, F. Relationship between the nanoporous texture of activated carbons and their capacitance properties in different electrolytes. *Carbon* **44**, 2498–2507 (2006).
39. Levi, M. D., Sigalov, S., Aurbach, D. & Daikhin, L. *In situ* electrochemical quartz crystal admittance methodology for tracking compositional and mechanical changes in porous carbon electrodes. *J. Phys. Chem. C* **117**, 14876–14889 (2013).
40. Levi, M. D., Salitra, G., Levy, N., Aurbach, D. & Maier, J. Application of a quartz-crystal microbalance to measure ionic fluxes in microporous carbons for energy storage. *Nature Mater.* **8**, 872–875 (2009).  
**This paper demonstrates that it is possible to monitor the gravimetric response of microporous carbons during the ion adsorption inside the pores.**
41. Sigalov, S., Levi, M. D., Daikhin, L., Salitra, G. & Aurbach, D. Electrochemical quartz crystal admittance studies of ion adsorption on nanoporous composite carbon electrodes in aprotic solutions. *J. Solid State Electrochem.* **18**, 1335–1344 (2014).
42. Ohkubo, T. *et al.* Restricted hydration structures of Rb and Br ions confined in slit-shaped carbon nanopore. *J. Am. Chem. Soc.* **124**, 11860–11861 (2002).  
**This paper shows that desolvation of aqueous ions occurs under extreme confinement using extended X-ray absorption fine structure experiments.**
43. Tsai, W.-Y., Taberna, P.-L. & Simon, P. Electrochemical quartz crystal microbalance (EQCM) study of ion dynamics in nanoporous carbons. *J. Am. Chem. Soc.* **136**, 8722–8728 (2014).
44. Fedorov, M. V. & Kornyshev, A. A. Ionic liquids at electrified interfaces. *Chem. Rev.* **114**, 2978–3036 (2014).
45. Xing, L., Vatamanu, J., Borodin, O. & Bedrov, D. On the atomistic nature of capacitance enhancement generated by ionic liquid electrolyte confined in subnanometer pores. *J. Phys. Chem. Lett.* **4**, 132–140 (2013).
46. Freise, V. Zur theorie der diffusendoppelschicht. *Z. Elektrochem.* **56**, 822–827 (1952).
47. Kornyshev, A. A. Double-layer in ionic liquids: paradigm change? *J. Phys. Chem. B* **111**, 5545–5557 (2007).
48. Limmer, D. T. *et al.* Charge fluctuations in nanoscale capacitors. *Phys. Rev. Lett.* **111**, 106102 (2013).
49. Merlet, C. *et al.* The electric double layer has a life of its own. *J. Phys. Chem. C* **118**, 18291–18298 (2014).
50. Kornyshev, A. A. & Qiao, R. Three-dimensional double layers. *J. Phys. Chem. C* **118**, 18285–18290 (2014).

51. Gebbie, M. A. *et al.* Ionic liquids behave as dilute electrolyte solutions. *Proc. Natl Acad. Sci. USA* **110**, 9674–9679 (2013).
52. Perkin, S., Salanne, M., Madden, P. & Lynden-Bell, R. Is a stern and diffuse layer model appropriate to ionic liquids at surfaces? *Proc. Natl Acad. Sci. USA* **110**, E4121 (2013).
53. Bozym, D. *et al.* Anomalous capacitance maximum of the glassy carbon–ionic liquid interface through dilution with organic solvents. *J. Phys. Chem. Lett.* **6**, 2644–2648 (2015).
54. Lee, A. A., Vella, D., Perkin, S. & Goriely, A. Are room-temperature ionic liquids dilute electrolyte? *J. Phys. Chem. Lett.* **6**, 159–163 (2015).
55. Bazant, M. Z., Storey, B. D. & Kornyshev, A. A. Double layer in ionic liquids: overscreening versus crowding. *Phys. Rev. Lett.* **106**, 046102 (2011).
56. Kondrat, S. & Kornyshev, A. A. Superionic state in double-layer capacitors with nanoporous electrodes. *J. Phys. Condens. Matter* **23**, 022201 (2011).  
**This paper explains the increase of capacitance in microporous carbons by the formation of image charges on the walls which screen the electrostatic interactions between the ions, leading to the formation of a 'superionic' state.**
57. Kondrat, S., Georgi, N., Fedorov, M. V. & Kornyshev, A. A. A superionic state in nano-porous double-layer capacitors: insights from Monte Carlo simulations. *Phys. Chem. Chem. Phys.* **13**, 11359–11366 (2011).
58. Griffin, J. M. *et al.* Ion counting in supercapacitor electrode using NMR spectroscopy. *Faraday Discuss.* **176**, 49–68 (2014).
59. Pean, C. *et al.* Confinement, desolvation and electrosorption effects on the diffusion of ions in nanoporous carbon electrodes. *J. Am. Chem. Soc.* **137**, 12627–12632 (2015).
60. Richey, F. W., Dyatkin, B., Gogotsi, Y. & Elabd, Y. A. Ion dynamics in porous carbon electrodes in supercapacitors using *in situ* infrared spectroelectrochemistry. *J. Am. Chem. Soc.* **135**, 12818–12826 (2013).
61. Prehal, C. *et al.* Tracking the structural arrangement of ions in carbon supercapacitor nanopores using *in-situ* small angle X-ray scattering. *Energy Environ. Sci.* **8**, 1725–1735 (2015).
62. Ilott, A. J., Trease, N. M., Grey, C. P. & Jerschow, A. Multinuclear *in situ* magnetic resonance imaging of electrochemical double-layer capacitors. *Nature Commun.* **5**, 4536 (2014).
63. Kondrat, S., Wu, P., Qiao, R. & Kornyshev, A. A. Accelerating charging dynamics in subnanometre pores. *Nature Mater.* **13**, 387–393 (2014).
64. He, Y. *et al.* The importance of ion packing on the dynamics of ionic liquids during micropore charging. *J. Phys. Chem. Lett.* **7**, 36–42 (2016).
65. Pean, C. *et al.* On the dynamics of charging in nanoporous carbon-based supercapacitors. *ACS Nano* **8**, 1576–1583 (2014).
66. Augustyn, C., Simon, P. & Dunn, B. Pseudocapacitive oxide materials for high-rate electrochemical energy storage. *Energy Environ. Sci.* **7**, 1597–1614 (2014).
67. Kim, J. W., Augustyn, V. & Dunn, B. The effect of crystallinity on the rapid pseudocapacitive response of Nb<sub>2</sub>O<sub>5</sub>. *Adv. Energy Mater.* **2**, 141–148 (2012).
68. Come, J. *et al.* Electrochemical kinetics of nanostructured Nb<sub>2</sub>O<sub>5</sub> electrodes. *J. Electrochem. Soc.* **161**, A718–A725 (2014).
69. Dmowski, W., Egami, T., Swider-Lyons, K. E., Love, C. T. & Rolison, D. R. Local atomic structure and conduction mechanism of nanocrystalline hydrous RuO<sub>2</sub> from X-ray scattering. *J. Phys. Chem. B* **106**, 12677–12683 (2002).
70. Augustyn, V. *et al.* High-rate electrochemical energy storage through Li<sup>+</sup> intercalation pseudocapacitance. *Nature Mater.* **12**, 518–522 (2013).  
**This paper reports on a pseudocapacitance mechanism based on lithium ion intercalation and defines the structural characteristics which are necessary for this process to occur.**
71. Brousse, T., Belanger, D. & Long, J. W. To be or not to be pseudocapacitive? *J. Electrochem. Soc.* **162**, A5185–A5189 (2015).
72. Kim, H.-S., Cook, J. B., Tolbert, S. H. & Dunn, B. The development of pseudocapacitive properties in nanosized-MoO<sub>2</sub>. *J. Electrochem. Soc.* **162**, A5083–A5090 (2015).
73. Simon, P., Gogotsi, Y. & Dunn, B. Where do batteries end and supercapacitors begin? *Science* **343**, 1210–1211 (2014).
74. Augustyn, V. *et al.* Lithium-ion storage properties of titanium oxide nanosheets. *Mater. Horiz.* **1**, 219–233 (2014).
75. Athouel, L. *et al.* Variation of the MnO<sub>2</sub> birnessite structure upon charge/discharge in an electrochemical supercapacitor electrode in aqueous Na<sub>2</sub>SO<sub>4</sub> electrolyte. *J. Phys. Chem. C* **112**, 7270–7277 (2008).
76. Wei, W., Cui, X., Chen, W. & Ivey, D. G. Manganese oxide-based materials as electrochemical supercapacitor electrodes. *Chem. Soc. Rev.* **40**, 1697–1721 (2011).
77. Ghodbane, O., Pascal, J.-L. & Favier, F. Microstructural effects on charge-storage properties in MnO<sub>2</sub>-based electrochemical supercapacitors. *ACS Appl. Mater. Interfaces* **1**, 1130–1139 (2009).
78. Ghodbane, O., Ataherian, F., Wu, N.-L. & Favier, F. *In situ* crystallographic investigations of charge storage mechanisms in MnO<sub>2</sub>-based electrochemical capacitors. *J. Power Sources* **206**, 454–462 (2012).
79. Rangom, Y., Tang, X. & Nazar, L. F. Carbon nanotube-based supercapacitors with excellent ac line filtering and rate capability via improved interfacial impedance. *ACS Nano* **9**, 7248–7255 (2015).
80. Zhu, Y. *et al.* A carbon quantum dot decorated RuO<sub>2</sub> network: outstanding supercapacitances under ultrafast charge and discharge. *Energy Environ. Sci.* **6**, 3665–3675 (2013).
81. Aravindan, V., Gnanaraj, J., Lee, Y. S. & Madhavi, S. Insertion-type electrodes for nonaqueous Li-ion capacitors. *Chem. Rev.* **114**, 11619–11635 (2014).
82. Naoi, K., Ishimoto, S., Isobe, Y. & Aoyagi, S. High-rate nano-crystalline Li<sub>4</sub>Ti<sub>5</sub>O<sub>12</sub> attached on carbon nano-fibers for hybrid supercapacitors. *J. Power Sources* **195**, 6250–6254 (2010).
83. Naoi, K., Ishimoto, S., Ogihara, N., Nakagawa, Y. & Hatta, S. Encapsulation of nanodot ruthenium oxide into KB for electrochemical capacitors. *J. Electrochem. Soc.* **156**, A52–A59 (2009).
84. Naoi, K., Ishimoto, S., Miyamoto, J. & Naoi, W. Second generation 'nanohybrid supercapacitor': evolution of capacitive energy storage devices. *Energy Environ. Sci.* **5**, 9363–9373 (2012).  
**This paper reports on the perspectives opened by combining a negative graphite electrode of a Li-ion battery with a capacitive porous-carbon positive electrode.**
85. Naoi, K., Naoi, W., Aoyagi, S., Miyamoto, J. & Kamino, T. New generation 'nanohybrid supercapacitor'. *Acc. Chem. Res.* **46**, 1075–1083 (2012).
86. Vatamanu, J. & Bedrov, D. Capacitive energy storage: current and future challenges. *J. Phys. Chem. Lett.* **6**, 3594–3609 (2015).
87. Lin, T. *et al.* Nitrogen-doped mesoporous carbon of extraordinary capacitance for electrochemical energy storage. *Science* **350**, 1508–1513 (2015).
88. Curtarolo, S. *et al.* The high-throughput highway to computational materials design. *Nature Mater.* **12**, 191–201 (2013).
89. Schutter, C., Husch, T., Korth, M. & Balducci, A. Toward new solvents for EDLCs: from computational screening to electrochemical validation. *J. Phys. Chem. C* **119**, 13413–13424 (2015).
90. Pognon, G., Brousse, T., Demarconnay, L. & Bélanger, D. Performance and stability of electrochemical capacitor based on anthraquinone modified activated carbon. *J. Power Sources* **196**, 4117–4122 (2011).
91. Abbas, Q. *et al.* Strategies to improve the performance of carbon/carbon capacitors in salt aqueous electrolytes. *J. Electrochem. Soc.* **162**, A5148–A5157 (2015).
92. Pohlmann, S. *et al.* Mixtures of azepanium based ionic liquids and propylene carbonate as high voltage electrolytes for supercapacitors. *Electrochim. Acta* **153**, 426–432 (2015).
93. Acerce, M., Voiry, D. & Chhowalla, M. Metallic 1T phase MoS<sub>2</sub> nanosheets as supercapacitor electrode materials. *Nature Nanotech.* **10**, 313–318 (2015).
94. Ghidoui, M., Lukatskaya, M. R., Zhao, M. Q., Gogotsi, Y. & Barsoum, M. W. Conductive two-dimensional titanium carbide 'clay' with high volumetric capacitance. *Nature* **516**, 78–81 (2014).
95. Shi, C. Y. *et al.* Structure of nanocrystalline Ti<sub>3</sub>C<sub>2</sub> MXene using atomic pair distribution function. *Phys. Rev. Lett.* **112**, 125501 (2014).
96. Levi, M. D. *et al.* Solving the capacitive paradox of 2D MXene using electrochemical quartz-crystal admittance and *in situ* electronic conductance measurements. *Adv. Energy Mater.* **5**, 1400815 (2015).
97. Soloveichik, G. L. Flow batteries: current status and trends. *Chem. Rev.* **115**, 11533–11558 (2015).
98. Kwon, C.-H. *et al.* High power biofuel cells textiles from woven bisrolled carbon nanotube yarns. *Nature Commun.* **5**, 3928 (2014).
99. Presser, V. *et al.* The electrochemical flow capacitor: a new concept for rapid energy storage and recovery. *Adv. Energy Mater.* **2**, 895–902 (2012).
100. Brogioli, D. Extracting renewable energy from a salinity difference using a capacitor. *Phys. Rev. Lett.* **103**, 058501 (2009).
101. Siria, A. *et al.* Giant osmotic energy conversion measured in a single transmembrane boron nitride nanotube. *Nature* **494**, 455–458 (2013).
102. Wang, J. Carbon nanotube based electrochemical biosensors. *Electroanalysis* **17**, 7–14 (2005).
103. Mirica, K. A., Azzarelli, J. M., Weis, J. G., Schnorr, J. M. & Swager, T. M. Rapid prototyping of carbon-based chemiresistive gas sensors on paper. *Proc. Natl Acad. Sci. USA* **110**, E3265–E3270 (2013).

## Acknowledgements

We thank our many co-workers who have contributed to the work presented in this review. C.P.G. thanks J. Griffin for his critical reading of the manuscript. The research leading to these results has received funding from the European Research Council under the European Union's Seventh Framework Programme (FP/2007-2013)/ ERC grant agreement no. 102539.

## Additional information

Reprints and permissions information is available online at [www.nature.com/reprints](http://www.nature.com/reprints). Correspondence should be addressed to P.S.

## Competing interests

The authors declare no competing financial interests.